Eur. Phys. J. C (2012) 72:2118
DOI 10.1140/epjc/s10052-012-2118-7

THE EUROPEAN PHYSICAL JOURNAL C

Regular Article - Experimental Physics

Measurement of relative branching fractions of B decays to $\psi(2S)$ and J/ψ mesons

The LHCb Collaboration[⋆]

CERN, 1211 Geneva 23, Switzerland

Received: 7 May 2012 / Revised: 6 July 2012 / Published online: 29 August 2012

Abstract The relative rates of B-meson decays into J/ψ and $\psi(2S)$ mesons are measured for the three decay modes in pp collisions recorded with the LHCb detector. The ratios of branching fractions ($\mathcal{B}$) are measured to be

$$\frac{\mathcal{B}(B^+ \to \psi(2S)K^+)}{\mathcal{B}(B^+ \to J/\psi K^+)} = 0.594 \pm 0.006(\text{stat}) \pm 0.016(\text{syst}) \pm 0.015(R_\psi),$$

$$\frac{\mathcal{B}(B^0 \to \psi(2S)K^{*0})}{\mathcal{B}(B^0 \to J/\psi K^{*0})} = 0.476 \pm 0.014(\text{stat}) \pm 0.010(\text{syst}) \pm 0.012(R_\psi),$$

$$\frac{\mathcal{B}(B_s^0 \to \psi(2S)\phi)}{\mathcal{B}(B_s^0 \to J/\psi\phi)} = 0.489 \pm 0.026(\text{stat}) \pm 0.021(\text{syst}) \pm 0.012(R_\psi),$$

where the third uncertainty is from the ratio of the $\psi(2S)$ and J/ψ branching fractions to $\mu^+\mu^-$.

1 Introduction

Decays of B mesons to two-body final states containing a charmonium resonance such as a J/ψ or $\psi(2S)$ offer a powerful way of studying electroweak transitions. Such decays probe charmonium properties and play a role in the study of CP violation and mixing in the neutral B system [1].

The relative branching fractions of B^+, B^0 and B_s^0 mesons into J/ψ and $\psi(2S)$ mesons have previously been studied by both the CDF and D0 collaborations [2–4]. Since the current experimental results for the study of CP violation in B_s^0 mixing using the $B_s^0 \to J/\psi\phi$ decay [5–7] are statistically limited, it is important to establish other channels where this analysis can be done. One such channel is the $B_s^0 \to \psi(2S)\phi$ decay.

In this paper, measurements of the ratios of the branching fractions of B mesons decaying to $\psi(2S)X$ and $J/\psi X$ are reported, where B denotes a B^+, B^0 or B_s^0 meson (charge conjugate decays are implicitly included) and X denotes a K^+, K^{*0} or ϕ meson. The data were collected by the LHCb experiment in pp collisions at the centre-of-mass energy $\sqrt{s} = 7$ TeV during 2011 and correspond to an integrated luminosity of 0.37 fb^{-1}.

2 Detector description

The LHCb detector [8] is a single-arm forward spectrometer covering the pseudorapidity range $2 < \eta < 5$, designed for the study of b- and c-hadrons. The detector includes a high precision tracking system consisting of a silicon-strip vertex detector surrounding the pp interaction region, a large-area silicon-strip detector located upstream of a dipole magnet with a bending power of about 4 Tm, and three stations of silicon-strip detectors and straw drift-tubes placed downstream. The combined tracking system has a momentum resolution $\Delta p/p$ that varies from 0.4 % at 5 GeV/c to 0.6 % at 100 GeV/c, and an impact parameter resolution of 20 μm for tracks with high transverse momentum. Data were taken with both magnet polarities to reduce systematic effects due to detector asymmetries. Charged hadrons are identified using two ring-imaging Cherenkov (RICH) detectors. Photon, electron and hadron candidates are identified by a calorimeter system consisting of scintillating-pad and pre-shower detectors, and electromagnetic and hadronic calorimeters. Muons are identified by a muon system composed of alternating layers of iron and multiwire proportional chambers. The trigger consists of a hardware stage based on information from the calorimeter and muon systems, followed by a software stage which applies a full event reconstruction.

Events with a $J/\psi \to \mu^+\mu^-$ final state are triggered using two hardware trigger decisions: the single-muon decision, which requires one muon candidate with a transverse momentum p_{T} larger than 1.5 GeV/c, and the dimuon decision, which requires two muon candidates with

⋆ e-mail: Ivan.Belyaev@cern.ch

transverse momenta p_{T_1} and p_{T_2} satisfying the relation $\sqrt{p_{T_1} \cdot p_{T_2}} > 1.3$ GeV/c. The di-muon trigger decision in the software trigger requires muon pairs of opposite charge with $p_T > 500$ MeV/c, forming a common vertex and with an invariant mass in excess of 2.9 GeV/c^2.

3 Event selection

In this analysis, the decays $B^+ \to \psi K^+ (B^0 \to \psi K^{*0}$, $B_s^0 \to \psi\phi)$ are reconstructed, where ψ represents $\psi(2S)$ or J/ψ, reconstructed in the $\psi \to \mu^+\mu^-$ decay modes. A $K^+(K^{*0}, \phi)$ candidate is added to the di-muon pair to form a $B^+(B^0, B_s^0)$ candidate.

The starting point of the analysis is the reconstruction of either a J/ψ or $\psi(2S)$ meson decaying into a di-muon pair. Candidates are formed from pairs of opposite sign tracks that both have a transverse momentum larger than 500 MeV/c. Good reconstruction quality is assured by requiring the χ^2 per degree of freedom of the track fit to satisfy $\chi^2/\text{ndf} < 5$. Both tracks must be identified as muons. This is achieved by requiring the muon identification variable, the difference in logarithm of the likelihood of the muon and hadron hypotheses [9] provided by the muon detection system, to satisfy $\Delta \log \mathcal{L}^{\mu-h} > -5$. The muons are required to form a common vertex of good quality ($\chi^2_{\text{vtx}} < 20$). The resulting di-muon candidate is required to have decay length significance from its associated primary vertex greater than 5 and have an invariant mass between 3020 and 3135 MeV/c^2 in the case of a J/ψ candidate or between 3597 and 3730 MeV/c^2 for a $\psi(2S)$ candidate. These correspond to $[-5\sigma; 3\sigma]$ windows around the nominal mass. The asymmetric window allows for the QED radiative tail.

The selected J/ψ and $\psi(2S)$ candidates are then combined with a K^+, K^{*0} or ϕ to create B meson candidates. Only the $K^{*0} \to K^+\pi^-$ and $\phi \to K^+K^-$ decay modes are considered. Pion-kaon separation is provided by the ring-imaging Cherenkov detectors. To identify kaons the difference in logarithm of the likelihood of the kaon and pion hypotheses [9] is required to satisfy $\Delta \log \mathcal{L}^{K-\pi} > -5$. In the case of pions the difference in logarithm of the likelihood of the pion and kaon hypotheses [9] is required to satisfy $\Delta \log \mathcal{L}^{\pi-K} > -5$. As in the case of muons, a cut is applied on the track χ^2/ndf provided by the track fit at 5. The kaons and pions are required to have a transverse momentum larger than 250 MeV/c and to have an impact parameter significance with respect to any primary vertex larger than 2. In the B^0 channel, the mass of the kaon and pion system is required to be $842 < \text{M}_{K^+\pi^-} < 942$ MeV/c^2 and in the B_s^0 channel the mass of the kaon pair is required to be $1010 < \text{M}_{K^+K^-} < 1030$ MeV/c^2.

In addition, we require the decay time of the B candidate ($c\tau$) to be larger than 100 μm to reduce the large combinatorial background from particles produced in the primary pp interaction. A global refit of the three-prong (four-prong) combination is performed with a primary vertex constraint and with the di-muon pair mass constrained to the nominal value [10] using the Decay Tree Fit (DTF) procedure [11]. The reduced χ^2 of this fit (χ^2_{DTF}/ndf) is required to be less than 5, where the DTF algorithm takes into account the number of decay products to determine the number of degrees of freedom. The B^+ candidates, where a muon from the $\psi(2S) \to \mu^+\mu^-$ decay is reconstructed as both muon and kaon, are removed by requiring the angle between the same sign muon and kaon to be greater than 3 mrad.

4 Measurement of $N_{\psi(2S)X}/N_{J/\psi X}$

The mass distributions for selected candidates are shown in Fig. 1. The number of the $B^+ \to \psi K^+$ candidates is estimated by performing an unbinned maximum likelihood fit. The same procedure is used to determine the number of the $B^0 \to \psi K^+\pi^-$ candidates in a $842 < \text{M}_{K^+\pi^-} < 942$ MeV/c^2 mass window and the number of the $B_s^0 \to \psi K^+K^-$ candidates in a $1010 < \text{M}_{K^+K^-} < 1030$ MeV/c^2 mass window. The number of signal candidates is determined by fitting a double-sided Crystal Ball function [12, 13] for signal together with an exponential function to model the background. The tail parameters of the Crystal Ball function are fixed to values determined from simulation.

To estimate the contribution from non-resonant decays $B^0 \to \psi K^+\pi^-$ and $B_s^0 \to \psi K^+K^-$, the $K^+\pi^-$ and K^+K^- invariant mass distributions have been studied after relaxing requirements on the $K^+\pi^-$ and K^+K^- invariant masses, see Fig. 2. The $K^+\pi^-$ and K^+K^- invariant mass distributions are then fitted with the sum of a relativistic Breit-Wigner function convolved with a Gaussian, to describe the resonant contribution from the K^{*0} or ϕ, two-body phase space function multiplied by a second order polynomial, to describe the non-resonant $K^+\pi^-$ or K^+K^- contribution. The *sPlot* technique [14] is used to unfold the $\psi K^+\pi^-$ or ψK^+K^- invariant mass of the non-resonant (in $K^+\pi^-$ and K^+K^-) candidates. This unfolded distribution contains a mixture of combinatorial background and non-resonant $B^0 \to \psi K^+\pi^-$ or $B_s^0 \to \psi K^+K^-$ decays. The invariant mass of the unfolded B candidates is shown in Fig. 3. The same function used in Fig. 1 is then used to estimate the contribution from the non-resonant B decays, which is subtracted from the total yield to estimate the contribution from resonant $B^0 \to \psi K^{*0}$ or $B_s^0 \to \psi\phi$ decays. The contribution of the resonant decays can also be extracted by unfolding the contribution of resonant $K^+\pi^-$ or K^+K^- decays to the $\psi K^+\pi^-$ or ψK^+K^- invariant mass distribution. This yields a compatible, but a statistically less precise, result. The yields are summarized listed in Table 1.

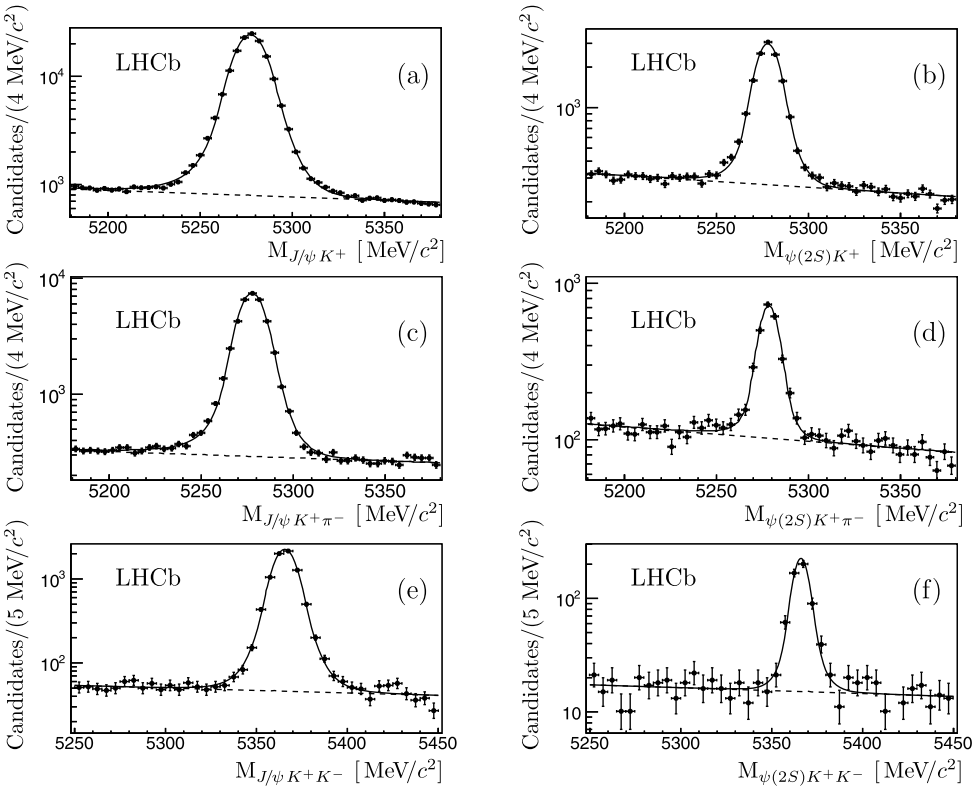

Fig. 1 Mass distributions of (**a**) $B^+ \to J/\psi K^+$, (**b**) $B^+ \to \psi(2S)K^+$, (**c**) $B^0 \to J/\psi K^+\pi^-$, (**d**) $B^0 \to \psi(2S)K^+\pi^-$, (**e**) $B_s^0 \to J/\psi K^+K^-$ and (**f**) $B_s^0 \to \psi(2S)K^+K^-$. The total fitted function (*solid*) and the combinatorial background (*dashed*) are shown. The variation in resolution of the different modes is fully consistent with the energy released in the decays and in agreement with simulation

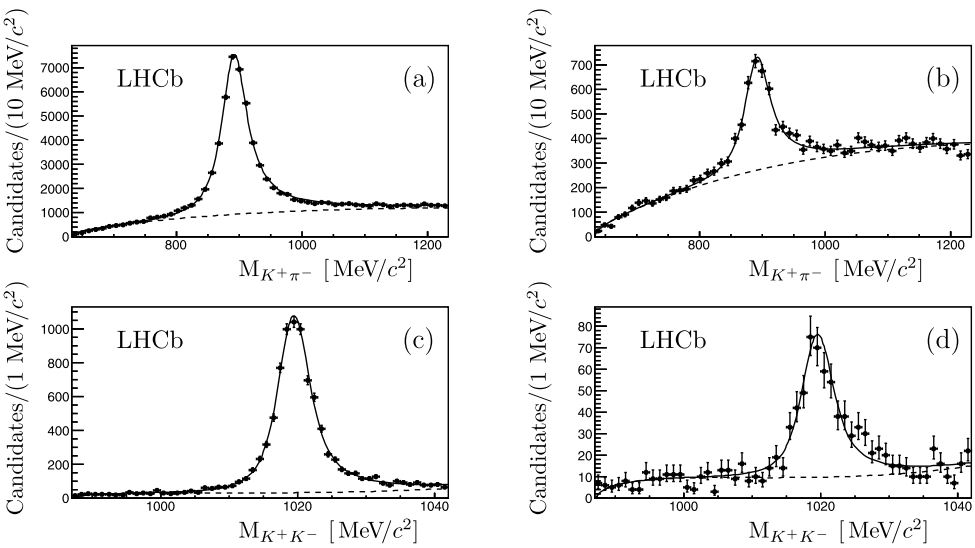

Fig. 2 Mass distributions of $K^+\pi^-$ or K^+K^- in (**a**) $B^0 \to J/\psi K^+\pi^-$, (**b**) $B^0 \to \psi(2S)K^+\pi^-$, (**c**) $B_s^0 \to J/\psi K^+K^-$ and (**d**) $B_s^0 \to \psi(2S)K^+K^-$ decays. The total fitted function (*solid*) and the combination of the non-resonant component and the combinatorial background (*dashed*) are shown. The fit is described in the text

5 Efficiencies and systematic uncertainties

The branching fraction ratio is calculated using

$$\frac{\mathcal{B}(B \to \psi(2S)X)}{\mathcal{B}(B \to J/\psi X)} = \frac{N^{\rm res}_{\psi(2S)X}}{N^{\rm res}_{J/\psi X}} \times \frac{\varepsilon_{J/\psi X}}{\varepsilon_{\psi(2S)X}} \times \frac{\mathcal{B}(J/\psi \to \mu^+\mu^-)}{\mathcal{B}(\psi(2S) \to \mu^+\mu^-)}, \quad (1)$$

where $N^{\rm res}$ is the number of signal candidates and ε is the overall efficiency.

The overall efficiency is the product of the geometrical acceptance of the detector, the combined reconstruction and selection efficiency, and the trigger efficiency. The efficiency ratio is estimated using simulation for all six modes. The simulation samples used are based on the PYTHIA 6.4 generator [15] configured with the parameters detailed in Ref. [16]. Final state QED radiative corrections are included using the PHOTOS package [17]. The EVTGEN [18] and GEANT4 [19] packages are used to generate hadron decays and simulate interactions in the detector, respectively. The

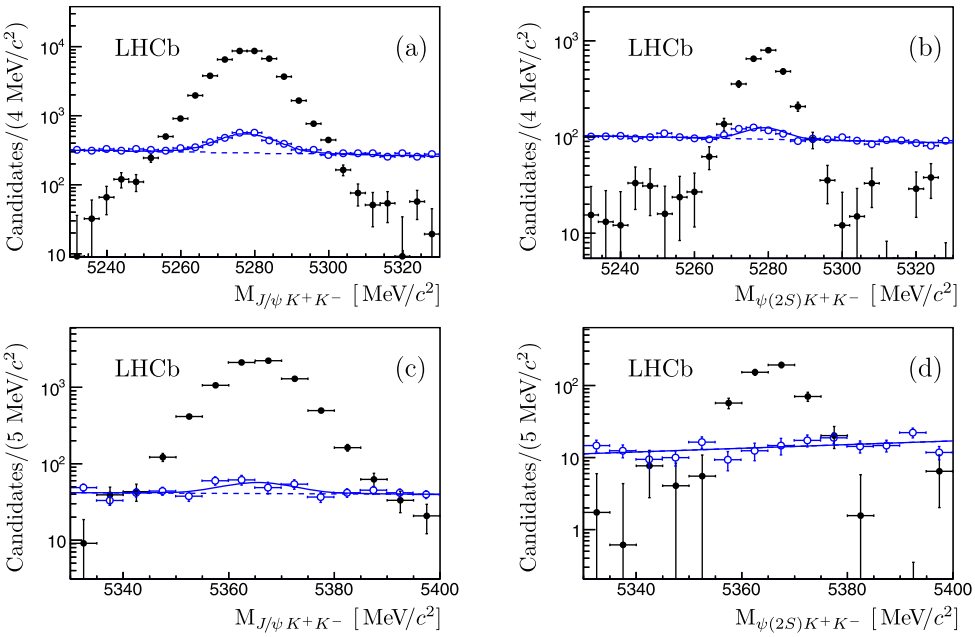

Fig. 3 Mass distributions of a (**a**) $B^0 \to J/\psi K^+\pi^-$, (**b**) $B^0 \to \psi(2S)K^+\pi^-$, (**c**) $B_s^0 \to J/\psi K^+K^-$ and (**d**) $B_s^0 \to \psi(2S)K^+K^-$ for resonant component (*full circles*) and non-resonant component (*open circles*). The total fitted function (*solid*) and the combinatorial background (*dashed*) are shown. The fit is described in the text

Table 1 Summary of the signal yields for the six B modes considered and the ratios of the number of J/ψ and $\psi(2S)$ decays: N^{total} is the summed signal yield for resonant and non-resonant modes, $N^{\text{non-res}}$ is the signal yield for non-resonant modes only and $N^{\text{res}}_{\psi X}$ is the signal yield for resonant decays (through K^{*0} or ϕ). The uncertainties are statistical only

B decay modes	N^{total}	$N^{\text{non-res}}$	N^{res}	$N^{\text{res}}_{\psi(2S)X}/N^{\text{res}}_{J/\psi X}$
$B^+ \to J/\psi K^+$	$141{,}769 \pm 410$	–	$141{,}769 \pm 410$	0.0857 ± 0.0009
$B^+ \to \psi(2S)K^+$	$12{,}154 \pm 130$	–	$12{,}154 \pm 130$	
$B^0 \to J/\psi K^+\pi^-$	$35{,}770 \pm 207$	$1{,}253 \pm 30$	$34{,}517 \pm 209$	0.0612 ± 0.0018
$B^0 \to \psi(2S)K^+\pi^-$	$2{,}223 \pm 60$	112 ± 12	$2{,}111 \pm 61$	
$B_s^0 \to J/\psi K^+K^-$	$7{,}654 \pm 92$	66 ± 13	$7{,}588 \pm 93$	0.0652 ± 0.0034
$B_s^0 \to \psi(2S)K^+K^-$	495 ± 25	0^{+1}_{-0}	495 ± 25	

digitized output is passed through a full simulation of both the hardware and software trigger and then reconstructed in the same way as the data.

The overall efficiency ratio is 0.901 ± 0.016, 1.011 ± 0.014 and 0.994 ± 0.014 for the B^+, the B^0 and the B_s^0 channels respectively. Since the selection criteria for $B \to J/\psi X$ and $B \to \psi(2S)X$ decays are identical, the ratio of efficiencies is expected to be close to unity. The deviation of the overall efficiency ratio from unity in the case of the $B^+ \to \psi K^+$ decays is due to the difference between the p_{T} spectra of muons for the J/ψ and $\psi(2S)$ decays. For the B^0 and B_s^0 channels this difference is small. It has been checked that the behaviour of the efficiencies of all selection criteria is consistent in the data and simulation.

Since the decay products in each of the pairs of channels considered have similar kinematics, most uncertainties cancel in the ratio. The different contributions to the systematic uncertainties affecting this analysis are discussed in the following and summarized in Table 2.

The dominant source of systematic uncertainty arises from the subtraction of the non-resonant components in the B^0 and the B_s^0 decays. The non-resonant background is studied with two alternative methods. First, determining the number of $B^0_{(s)} \to \psi K^{*0}(\phi)$ decays directly using the *sPlot* technique by unfolding and fitting the $B^0_{(s)}$ mass distribution

Table 2 Systematic uncertainties (in %) on the relative branching fractions

Source	B^+ channel	B^0 channel	B_s^0 channel
Non-resonant decays	—	1.5	3.4
Data-simulation agreement	1.7	0.5	2.0
Magnet polarity	1.4	0.6	0.7
Finite simulation sample size	0.3	0.5	0.6
Trigger	1.1	1.1	1.1
Background shape	0.6	0.2	0.2
Signal shape	0.7	0.8	0.5
Angular distribution	–	<0.1	0.6
Particle misidentification	0.4	<0.1	<0.1
Sum in quadrature	2.7	2.2	4.3

of candidates containing genuine $K^{*0}(\phi)$ resonances. Second, using the $B^0_{(s)}$ mass distribution as the discriminating variable to unfold the $K^+\pi^-(K^+K^-)$ mass distribution of genuine $B^0_{(s)}$ candidates and fitting this distribution to determine the number of non-resonant decays. The corresponding uncertainties are found to be 1.5 % in the B^0 channel and 3.4 % in the B^0_s channel.

The other important source of uncertainty arises from the estimation of the efficiencies due to the potential disagreement between data and simulation. This is studied by varying independently selection criteria in data and simulation. The corresponding uncertainties are found to be 1.7 % in the B^+ channel, 0.5 % in the B^0 channel and 2.0 % in the B^0_s channel. The observed difference in the efficiency ratios for the two magnet polarities is conservatively taken as an estimate of the systematic uncertainty. This is 1.4 % in the B^+ channel, 0.6 % in the B^0 channel and 0.7 % in the B^0_s channel.

The trigger is highly efficient in selecting B meson decays with two muons in the final state. For this analysis the di-muon pair is required to trigger the event. Differences in the trigger efficiency between data and simulation are studied in the data using events which were triggered independently on the di-muon pair [20]. Based on these studies, an uncertainty of 1.1 % is assigned.

A further uncertainty arises from the imperfect knowledge of the shape of the signal and background in the B meson mass distribution. To estimate this effect, a linear and a quadratic function are considered as alternative models for the background mass distribution. In addition, a double Gaussian shape and a sum of double-sided Crystal Ball and Gaussian shapes are used as alternative models for the signal shape. The maximum observed change in the ratio of yields in the $\psi(2S)$ and J/ψ modes is taken as systematic uncertainty.

The central value of the relative efficiency is determined by assuming that the angular distribution of the $B \to \psi(2S)X$ decay is the same as that of the $B \to J/\psi X$. The systematic uncertainty due to the unknown polarization of the $\psi(2S)$ in the B meson decays is estimated as follows. The simulation samples were re-weighted to match the angular distributions found from the data and the relative efficiency was recalculated. The difference between the baseline analysis and the re-weighted simulation is taken as the systematic uncertainty, as shown in Table 2.

Finally, the uncertainty due to potential contribution from the Cabibbo-suppressed mode with a π misidentified as K is found to be 0.4 % in the B^+ channel and negligible in the B^0 and B^0_s channels. The uncertainty due to the cross-feed between B^0 and B^0_s channels with a π misidentified as K (or a K misidentified as π) is negligible.

6 Results

Since the di-electron branching fractions are measured more precisely than those of the di-muon decay modes, we assume lepton universality and take $R_\psi = \mathcal{B}(J/\psi \to \mu^+\mu^-)/\mathcal{B}(\psi(2S) \to \mu^+\mu^-) = \mathcal{B}(J/\psi \to e^+e^-)/\mathcal{B}(\psi(2S) \to e^+e^-) = 7.69 \pm 0.19$ [10]. The results are combined using Eq. (1) to give

$$\frac{\mathcal{B}(B^+ \to \psi(2S)K^+)}{\mathcal{B}(B^+ \to J/\psi K^+)} = 0.594 \pm 0.006(\text{stat}) \pm 0.016(\text{syst}) \pm 0.015(R_\psi),$$

$$\frac{\mathcal{B}(B^0 \to \psi(2S)K^{*0})}{\mathcal{B}(B^0 \to J/\psi K^{*0})} = 0.476 \pm 0.014(\text{stat}) \pm 0.010(\text{syst}) \pm 0.012(R_\psi),$$

$$\frac{\mathcal{B}(B^0_s \to \psi(2S)\phi)}{\mathcal{B}(B^0_s \to J/\psi\phi)} = 0.489 \pm 0.026(\text{stat}) \pm 0.021(\text{syst}) \pm 0.012(R_\psi),$$

where the first uncertainty is statistical, the second is systematic and the third is the uncertainty on the R_ψ value [10].

The resulting branching fraction ratios are compatible with, but significantly more precise than, the current world averages of $\mathcal{B}(B^+ \to \psi(2S)K^+)/\mathcal{B}(B^+ \to J/\psi K^+) = 0.60 \pm 0.07$ and $\mathcal{B}(B^0_s \to \psi(2S)\phi)/\mathcal{B}(B^0_s \to J/\psi\phi) = 0.53 \pm 0.10$ [10] and the CDF result of $\mathcal{B}(B^0 \to \psi(2S)K^{*0})/\mathcal{B}(B^0 \to J/\psi K^{*0}) = 0.515 \pm 0.113 \pm 0.052$ [2]. The $B^0_s \to \psi(2S)\phi$ decay is particularly interesting since, with more data, it can be used for the measurement of CP violation in B^0_s mixing.

Acknowledgements We express our gratitude to our colleagues in the CERN accelerator departments for the excellent performance of the LHC. We thank the technical and administrative staff at CERN and at the LHCb institutes, and acknowledge support from the National Agencies: CAPES, CNPq, FAPERJ and FINEP (Brazil); CERN; NSFC (China); CNRS/IN2P3 (France); BMBF, DFG, HGF and MPG (Germany); SFI (Ireland); INFN (Italy); FOM and NWO (The Netherlands); SCSR (Poland); ANCS (Romania); MinES of Russia and Rosatom (Russia); MICINN, XuntaGal and GENCAT (Spain); SNSF and SER (Switzerland); NAS Ukraine (Ukraine); STFC (United Kingdom); NSF (USA). We also acknowledge the support received from the ERC under FP7 and the Region Auvergne.

References

1. I.I.Y. Bigi, A.I. Sanda, Notes on the observability of *CP* violations in *B* decays. Nucl. Phys. B **193**, 85 (1981)
2. F. Abe et al. (CDF collaboration), Observation of $B^+ \to \psi(2S)K^+$ and $B^0 \to \psi(2S)K^*(892)^0$ decays and measurements of B-meson branching fractions into J/ψ and $\psi(2S)$ final states. Phys. Rev. D **58**, 072001 (1998). arXiv:hep-ex/9803013

3. A. Abulencia et al. (CDF collaboration), Observation of $B_s^0 \to \psi(2S)\phi$ and measurement of ratio of branching fractions $\mathcal{B}(B_s^0 \to \psi(2S)\phi)/\mathcal{B}(B_s^0 \to J/\psi\phi)$. Phys. Rev. Lett. **96**, 231801 (2006). arXiv:hep-ex/0602005
4. V. Abazov et al. (D0 collaboration), Relative rates of B meson decays into $\psi(2S)$ and J/ψ mesons. Phys. Rev. D **79**, 111102(R) (2009). arXiv:0805.2576
5. T. Aaltonen et al. (CDF collaboration), Measurement of CP violating phase β_s in $B_s^0 \to J/\psi\phi$ decays with the CDF II detector. Phys. Rev. D., submitted. arXiv:1112.1726
6. V.M. Abazov et al. (D0 Collaboration), Measurement of the CP-violating phase $\phi_s^{J/\psi\phi}$ using the flavor-tagged decay $B_s^0 \to J/\psi\phi$ in 8 fb^{-1} of $p\bar{p}$ collisions. Phys. Rev. D **85**, 032006 (2012). arXiv:1109.3166
7. R. Aaij et al. (LHCb collaboration), Measurement of the *CP*-violating phase ϕ_s in the decay $B_s^0 \to J/\psi\phi$. arXiv:1112.3183
8. A.A. Alves Jr. et al. (LHCb collaboration), The LHCb detector at the LHC. J. Instrum. **3**, S08005 (2008)
9. A. Powell et al., Particle identification at LHCb. PoS **ICHEP2010**, 020 (2010). LHCb-PROC-2011-008
10. K. Nakamura et al. (Particle Data Group), Review of particle physics. J. Phys. G **37**, 075021 (2010)
11. W. Hulsbergen, Decay chain fitting with Kalman filter. Nucl. Instrum. Methods A **552**, 566 (2005). arXiv:physics/0503191v1
12. T. Skwarnicki, A study of the radiative cascade transitions between the Upsilon-prime and Upsilon resonances. PhD thesis, Institute of Nuclear Physics, Krakow, 1986. DESY-F31-86-02
13. R. Aaij et al. (LHCb collaboration), Observation of J/ψ pair production in pp collisions at $\sqrt{s} = 7$ TeV. Phys. Lett. B **707**, 52 (2012). arXiv:1109.0963
14. M. Pivk, F.R. Le Diberder, sPlot: a statistical tool to unfold data distributions. Nucl. Instrum. Methods A **555**, 356 (2005). arXiv:physics/0402083v3
15. T. Sjöstrand, S. Mrenna, P. Skands, PYTHIA 6.4 physics and manual. J. High Energy Phys. **05**, 026 (2006). arXiv:hep-ph/0603175
16. I. Belyaev et al., Handling of the generation of primary events in GAUSS, the LHCb simulation framework, in *Nuclear Science Symposium Conference Record (NSS/MIC)* (IEEE, New York, 2010), p. 1155
17. P. Golonka, Z. Was, PHOTOS Monte Carlo: a precision tool for QED corrections in Z and W decays. Eur. Phys. J. C **45**, 97 (2006). arXiv:hep-ph/0506026
18. D.J. Lange, The EvtGen particle decay simulation package. Nucl. Instrum. Methods A **462**, 152 (2001)
19. S. Agostinelli et al. (GEANT4 collaboration), GEANT4: a simulation toolkit. Nucl. Instrum. Methods A **506**, 250 (2003)
20. V. Gligorov, C. Thomas, M. Williams, The HLT inclusive *B* triggers. LHCb-PUB-2011-016

The LHCb Collaboration

R. Aaij[38], C. Abellan Beteta[33,n], A. Adametz[11], B. Adeva[34], M. Adinolfi[43], C. Adrover[6], A. Affolder[49], Z. Ajaltouni[5], J. Albrecht[35], F. Alessio[35], M. Alexander[48], S. Ali[38], G. Alkhazov[27], P. Alvarez Cartelle[34], A.A. Alves Jr[22], S. Amato[2], Y. Amhis[36], J. Anderson[37], R.B. Appleby[51], O. Aquines Gutierrez[10], F. Archilli[18,35], A. Artamonov[32], M. Artuso[53,35], E. Aslanides[6], G. Auriemma[22,m], S. Bachmann[11], J.J. Back[45], V. Balagura[28,35], W. Baldini[16], R.J. Barlow[51], C. Barschel[35], S. Barsuk[7], W. Barter[44], A. Bates[48], C. Bauer[10], Th. Bauer[38], A. Bay[36], J. Beddow[48], I. Bediaga[1], S. Belogurov[28], K. Belous[32], I. Belyaev[28], E. Ben-Haim[8], M. Benayoun[8], G. Bencivenni[18], S. Benson[47], J. Benton[43], R. Bernet[37], M.-O. Bettler[17], M. van Beuzekom[38], A. Bien[11], S. Bifani[12], T. Bird[51], A. Bizzeti[17,h], P.M. Bjørnstad[51], T. Blake[35], F. Blanc[36], C. Blanks[50], J. Blouw[11], S. Blusk[53], A. Bobrov[31], V. Bocci[22], A. Bondar[31], N. Bondar[27], W. Bonivento[15], S. Borghi[48,51], A. Borgia[53], T.J.V. Bowcock[49], C. Bozzi[16], T. Brambach[9], J. van den Brand[39], J. Bressieux[36], D. Brett[51], M. Britsch[10], T. Britton[53], N.H. Brook[43], H. Brown[49], A. Büchler-Germann[37], I. Burducea[26], A. Bursche[37], J. Buytaert[35], S. Cadeddu[15], O. Callot[7], M. Calvi[20,j], M. Calvo Gomez[33,n], A. Camboni[33], P. Campana[18,35], A. Carbone[14], G. Carboni[21,k], R. Cardinale[19,35,i], A. Cardini[15], L. Carson[50], K. Carvalho Akiba[2], G. Casse[49], M. Cattaneo[35], Ch. Cauet[9], M. Charles[52], Ph. Charpentier[35], N. Chiapolini[37], M. Chrzaszcz[23], K. Ciba[35], X. Cid Vidal[34], G. Ciezarek[50], P.E.L. Clarke[47], M. Clemencic[35], H.V. Cliff[44], J. Closier[35], C. Coca[26], V. Coco[38], J. Cogan[6], E. Cogneras[5], P. Collins[35], A. Comerma-Montells[33], A. Contu[52], A. Cook[43], M. Coombes[43], G. Corti[35], B. Couturier[35], G.A. Cowan[36], R. Currie[47], C. D'Ambrosio[35], P. David[8], P.N.Y. David[38], I. De Bonis[4], K. De Bruyn[38], S. De Capua[21,k], M. De Cian[37], J.M. De Miranda[1], L. De Paula[2], P. De Simone[18], D. Decamp[4], M. Deckenhoff[9], H. Degaudenzi[36,35], L. Del Buono[8], C. Deplano[15], D. Derkach[14,35], O. Deschamps[5], F. Dettori[39], J. Dickens[44], H. Dijkstra[35], P. Diniz Batista[1], F. Domingo Bonal[33,n], S. Donleavy[49], F. Dordei[11], A. Dosil Suárez[34], D. Dossett[45], A. Dovbnya[40], F. Dupertuis[36], R. Dzhelyadin[32], A. Dziurda[23], A. Dzyuba[27], S. Easo[46], U. Egede[50], V. Egorychev[28], S. Eidelman[31], D. van Eijk[38], F. Eisele[11], S. Eisenhardt[47], R. Ekelhof[9], L. Eklund[48], Ch. Elsasser[37], D. Elsby[42], D. Esperante Pereira[34], A. Falabella[16,14,e], C. Färber[11], G. Fardell[47], C. Farinelli[38], S. Farry[12], V. Fave[36], V. Fernandez Albor[34], M. Ferro-Luzzi[35], S. Filippov[30], C. Fitzpatrick[47], M. Fontana[10], F. Fontanelli[19,i], R. Forty[35], O. Francisco[2], M. Frank[35], C. Frei[35], M. Frosini[17,f], S. Furcas[20], A. Gallas Torreira[34], D. Galli[14,c], M. Gandelman[2], P. Gandini[52], Y. Gao[3], J-C. Garnier[35], J. Garofoli[53], J. Garra Tico[44], L. Garrido[33], D. Gascon[33], C. Gaspar[35], R. Gauld[52], N. Gauvin[36], M. Gersabeck[35], T. Gershon[45,35], Ph. Ghez[4], V. Gibson[44], V.V. Gligorov[35], C. Göbel[54,p], D. Golubkov[28], A. Golutvin[50,28,35], A. Gomes[2], H. Gordon[52], M. Grabalosa Gándara[33], R. Graciani Diaz[33], L.A. Granado Cardoso[35], E. Graugés[33], G. Graziani[17], A. Grecu[26],

E. Greening[52], S. Gregson[44], O. Grünberg[55,q], B. Gui[53], E. Gushchin[30], Yu. Guz[32], T. Gys[35], C. Hadjivasiliou[53], G. Haefeli[36], C. Haen[35], S.C. Haines[44], T. Hampson[43], S. Hansmann-Menzemer[11], N. Harnew[52], J. Harrison[51], P.F. Harrison[45], T. Hartmann[55,q], J. He[7], V. Heijne[38], K. Hennessy[49], P. Henrard[5], J.A. Hernando Morata[34], E. van Herwijnen[35], E. Hicks[49], P. Hopchev[4], W. Hulsbergen[38], P. Hunt[52], T. Huse[49], R.S. Huston[12], D. Hutchcroft[49], D. Hynds[48], V. Iakovenko[41], P. Ilten[12], J. Imong[43], R. Jacobsson[35], A. Jaeger[11], M. Jahjah Hussein[5], E. Jans[38], F. Jansen[38], P. Jaton[36], B. Jean-Marie[7], F. Jing[3], M. John[52], D. Johnson[52], C.R. Jones[44], B. Jost[35], M. Kaballo[9], S. Kandybei[40], M. Karacson[35], T.M. Karbach[9], J. Keaveney[12], I.R. Kenyon[42], U. Kerzel[35], T. Ketel[39], A. Keune[36], B. Khanji[6], Y.M. Kim[47], M. Knecht[36], I. Komarov[29], R.F. Koopman[39], P. Koppenburg[38], M. Korolev[29], A. Kozlinskiy[38], L. Kravchuk[30], K. Kreplin[11], M. Kreps[45], G. Krocker[11], P. Krokovny[31], F. Kruse[9], K. Kruzelecki[35], M. Kucharczyk[20,23,35,j], V. Kudryavtsev[31], T. Kvaratskheliya[28,35], V.N. La Thi[36], D. Lacarrere[35], G. Lafferty[51], A. Lai[15], D. Lambert[47], R.W. Lambert[39], E. Lanciotti[35], G. Lanfranchi[18], C. Langenbruch[35], T. Latham[45], C. Lazzeroni[42], R. Le Gac[6], J. van Leerdam[38], J.-P. Lees[4], R. Lefèvre[5], A. Leflat[29,35], J. Lefrançois[7], O. Leroy[6], T. Lesiak[23], L. Li[3], Y. Li[3], L. Li Gioi[5], M. Lieng[9], M. Liles[49], R. Lindner[35], C. Linn[11], B. Liu[3], G. Liu[35], J. von Loeben[20], J.H. Lopes[2], E. Lopez Asamar[33], N. Lopez-March[36], H. Lu[3], J. Luisier[36], A. Mac Raighne[48], F. Machefert[7], I.V. Machikhiliyan[4,28], F. Maciuc[10], O. Maev[27,35], J. Magnin[1], S. Malde[52], R.M.D. Mamunur[35], G. Manca[15,d], G. Mancinelli[6], N. Mangiafave[44], U. Marconi[14], R. Märki[36], J. Marks[11], G. Martellotti[22], A. Martens[8], L. Martin[52], A. Martín Sánchez[7], M. Martinelli[38], D. Martinez Santos[35], A. Massafferri[1], Z. Mathe[12], C. Matteuzzi[20], M. Matveev[27], E. Maurice[6], B. Maynard[53], A. Mazurov[16,30,35], G. McGregor[51], R. McNulty[12], M. Meissner[11], M. Merk[38], J. Merkel[9], S. Miglioranzi[35], D.A. Milanes[13], M.-N. Minard[4], J. Molina Rodriguez[54,p], S. Monteil[5], D. Moran[12], P. Morawski[23], R. Mountain[53], I. Mous[38], F. Muheim[47], K. Müller[37], R. Muresan[26], B. Muryn[24], B. Muster[36], J. Mylroie-Smith[49], P. Naik[43], T. Nakada[36], R. Nandakumar[46], I. Nasteva[1], M. Needham[47], N. Neufeld[35], A.D. Nguyen[36], C. Nguyen-Mau[36,o], M. Nicol[7], V. Niess[5], N. Nikitin[29], T. Nikodem[11], A. Nomerotski[52,35], A. Novoselov[32], A. Oblakowska-Mucha[24], V. Obraztsov[32], S. Oggero[38], S. Ogilvy[48], O. Okhrimenko[41], R. Oldeman[15,35,d], M. Orlandea[26], J.M. Otalora Goicochea[2], P. Owen[50], B.K. Pal[53], J. Palacios[37], A. Palano[13,b], M. Palutan[18], J. Panman[35], A. Papanestis[46], M. Pappagallo[48], C. Parkes[51], C.J. Parkinson[50], G. Passaleva[17], G.D. Patel[49], M. Patel[50], S.K. Paterson[50], G.N. Patrick[46], C. Patrignani[19,i], C. Pavel-Nicorescu[26], A. Pazos Alvarez[34], A. Pellegrino[38], G. Penso[22,l], M. Pepe Altarelli[35], S. Perazzini[14,c], D.L. Perego[20,j], E. Perez Trigo[34], A. Pérez-Calero Yzquierdo[33], P. Perret[5], M. Perrin-Terrin[6], G. Pessina[20], A. Petrolini[19,i], A. Phan[53], E. Picatoste Olloqui[33], B. Pie Valls[33], B. Pietrzyk[4], T. Pilař[45], D. Pinci[22], R. Plackett[48], S. Playfer[47], M. Plo Casasus[34], G. Polok[23], A. Poluektov[45,31], I. Polyakov[28], E. Polycarpo[2], D. Popov[10], B. Popovici[26], C. Potterat[33], A. Powell[52], J. Prisciandaro[36], V. Pugatch[41], A. Puig Navarro[33], W. Qian[53], J.H. Rademacker[43], B. Rakotomiaramanana[36], M.S. Rangel[2], I. Raniuk[40], G. Raven[39], S. Redford[52], M.M. Reid[45], A.C. dos Reis[1], S. Ricciardi[46], A. Richards[50], K. Rinnert[49], D.A. Roa Romero[5], P. Robbe[7], E. Rodrigues[48,51], F. Rodrigues[2], P. Rodriguez Perez[34], G.J. Rogers[44], S. Roiser[35], V. Romanovsky[32], M. Rosello[33,n], J. Rouvinet[36], T. Ruf[35], H. Ruiz[33], G. Sabatino[21,k], J.J. Saborido Silva[34], N. Sagidova[27], P. Sail[48], B. Saitta[15,d], C. Salzmann[37], M. Sannino[19,i], R. Santacesaria[22], C. Santamarina Rios[34], R. Santinelli[35], E. Santovetti[21,k], M. Sapunov[6], A. Sarti[18,l], C. Satriano[22,m], A. Satta[21], M. Savrie[16,e], D. Savrina[28], P. Schaack[50], M. Schiller[39], H. Schindler[35], S. Schleich[9], M. Schlupp[9], M. Schmelling[10], B. Schmidt[35], O. Schneider[36], A. Schopper[35], M.-H. Schune[7], R. Schwemmer[35], B. Sciascia[18], A. Sciubba[18,l], M. Seco[34], A. Semennikov[28], K. Senderowska[24], I. Sepp[50], N. Serra[37], J. Serrano[6], P. Seyfert[11], M. Shapkin[32], I. Shapoval[40,35], P. Shatalov[28], Y. Shcheglov[27], T. Shears[49], L. Shekhtman[31], O. Shevchenko[40], V. Shevchenko[28], A. Shires[50], R. Silva Coutinho[45], T. Skwarnicki[53], N.A. Smith[49], E. Smith[52,46], M. Smith[51], K. Sobczak[5], F.J.P. Soler[48], A. Solomin[43], F. Soomro[18,35], B. Souza De Paula[2], B. Spaan[9], A. Sparkes[47], P. Spradlin[48], F. Stagni[35], S. Stahl[11], O. Steinkamp[37], S. Stoica[26], S. Stone[53,35], B. Storaci[38], M. Straticiuc[26], U. Straumann[37], V.K. Subbiah[35], S. Swientek[9], M. Szczekowski[25], P. Szczypka[36], T. Szumlak[24], S. T'Jampens[4], E. Teodorescu[26], F. Teubert[35], C. Thomas[52], E. Thomas[35], J. van Tilburg[11], V. Tisserand[4], M. Tobin[37], S. Tolk[39], S. Topp-Joergensen[52], N. Torr[52], E. Tournefier[4,50], S. Tourneur[36], M.T. Tran[36], A. Tsaregorodtsev[6], N. Tuning[38], M. Ubeda Garcia[35], A. Ukleja[25], U. Uwer[11], V. Vagnoni[14], G. Valenti[14], R. Vazquez Gomez[33], P. Vazquez Regueiro[34], S. Vecchi[16], J.J. Velthuis[43], M. Veltri[17,g], B. Viaud[7], I. Videau[7], D. Vieira[2], X. Vilasis-Cardona[33,n], J. Visniakov[34], A. Vollhardt[37], D. Volyanskyy[10], D. Voong[43], A. Vorobyev[27], V. Vorobyev[31], C. Voß[55,q], H. Voss[10], R. Waldi[55,q], R. Wallace[12], S. Wandernoth[11], J. Wang[53], D.R. Ward[44], N.K. Watson[42], A.D. Webber[51], D. Websdale[50], M. Whitehead[45], J. Wicht[35], D. Wiedner[11], L. Wiggers[38], G. Wilkinson[52], M.P. Williams[45,46], M. Williams[50], F.F. Wilson[46], J. Wishahi[9], M. Witek[23], W. Witzeling[35], S.A. Wotton[44], S. Wright[44], S. Wu[3], K. Wyllie[35], Y. Xie[47], F. Xing[52], Z. Xing[53], Z. Yang[3], R. Young[47], X. Yuan[3], O. Yushchenko[32], M. Zangoli[14], M. Zavertyaev[10,a], F. Zhang[3], L. Zhang[53], W.C. Zhang[12], Y. Zhang[3], A. Zhelezov[11], L. Zhong[3], A. Zvyagin[35]

[1]Centro Brasileiro de Pesquisas Físicas (CBPF), Rio de Janeiro, Brazil
[2]Universidade Federal do Rio de Janeiro (UFRJ), Rio de Janeiro, Brazil
[3]Center for High Energy Physics, Tsinghua University, Beijing, China

[4]LAPP, Université de Savoie, CNRS/IN2P3, Annecy-Le-Vieux, France
[5]Clermont Université, Université Blaise Pascal, CNRS/IN2P3, LPC, Clermont-Ferrand, France
[6]CPPM, Aix-Marseille Université, CNRS/IN2P3, Marseille, France
[7]LAL, Université Paris-Sud, CNRS/IN2P3, Orsay, France
[8]LPNHE, Université Pierre et Marie Curie, Université Paris Diderot, CNRS/IN2P3, Paris, France
[9]Fakultät Physik, Technische Universität Dortmund, Dortmund, Germany
[10]Max-Planck-Institut für Kernphysik (MPIK), Heidelberg, Germany
[11]Physikalisches Institut, Ruprecht-Karls-Universität Heidelberg, Heidelberg, Germany
[12]School of Physics, University College Dublin, Dublin, Ireland
[13]Sezione INFN di Bari, Bari, Italy
[14]Sezione INFN di Bologna, Bologna, Italy
[15]Sezione INFN di Cagliari, Cagliari, Italy
[16]Sezione INFN di Ferrara, Ferrara, Italy
[17]Sezione INFN di Firenze, Firenze, Italy
[18]Laboratori Nazionali dell'INFN di Frascati, Frascati, Italy
[19]Sezione INFN di Genova, Genova, Italy
[20]Sezione INFN di Milano Bicocca, Milano, Italy
[21]Sezione INFN di Roma Tor Vergata, Roma, Italy
[22]Sezione INFN di Roma La Sapienza, Roma, Italy
[23]Henryk Niewodniczanski Institute of Nuclear Physics Polish Academy of Sciences, Kraków, Poland
[24]AGH University of Science and Technology, Kraków, Poland
[25]Soltan Institute for Nuclear Studies, Warsaw, Poland
[26]Horia Hulubei National Institute of Physics and Nuclear Engineering, Bucharest-Magurele, Romania
[27]Petersburg Nuclear Physics Institute (PNPI), Gatchina, Russia
[28]Institute of Theoretical and Experimental Physics (ITEP), Moscow, Russia
[29]Institute of Nuclear Physics, Moscow State University (SINP MSU), Moscow, Russia
[30]Institute for Nuclear Research of the Russian Academy of Sciences (INR RAN), Moscow, Russia
[31]Budker Institute of Nuclear Physics (SB RAS) and Novosibirsk State University, Novosibirsk, Russia
[32]Institute for High Energy Physics (IHEP), Protvino, Russia
[33]Universitat de Barcelona, Barcelona, Spain
[34]Universidad de Santiago de Compostela, Santiago de Compostela, Spain
[35]European Organization for Nuclear Research (CERN), Geneva, Switzerland
[36]Ecole Polytechnique Fédérale de Lausanne (EPFL), Lausanne, Switzerland
[37]Physik-Institut, Universität Zürich, Zürich, Switzerland
[38]Nikhef National Institute for Subatomic Physics, Amsterdam, The Netherlands
[39]Nikhef National Institute for Subatomic Physics and VU University Amsterdam, Amsterdam, The Netherlands
[40]NSC Kharkiv Institute of Physics and Technology (NSC KIPT), Kharkiv, Ukraine
[41]Institute for Nuclear Research of the National Academy of Sciences (KINR), Kyiv, Ukraine
[42]University of Birmingham, Birmingham, United Kingdom
[43]H.H. Wills Physics Laboratory, University of Bristol, Bristol, United Kingdom
[44]Cavendish Laboratory, University of Cambridge, Cambridge, United Kingdom
[45]Department of Physics, University of Warwick, Coventry, United Kingdom
[46]STFC Rutherford Appleton Laboratory, Didcot, United Kingdom
[47]School of Physics and Astronomy, University of Edinburgh, Edinburgh, United Kingdom
[48]School of Physics and Astronomy, University of Glasgow, Glasgow, United Kingdom
[49]Oliver Lodge Laboratory, University of Liverpool, Liverpool, United Kingdom
[50]Imperial College London, London, United Kingdom
[51]School of Physics and Astronomy, University of Manchester, Manchester, United Kingdom
[52]Department of Physics, University of Oxford, Oxford, United Kingdom
[53]Syracuse University, Syracuse, NY, United States
[54]Pontifícia Universidade Católica do Rio de Janeiro (PUC-Rio), Rio de Janeiro, Brazil
[55]Institut für Physik, Universität Rostock, Rostock, Germany
[a]P.N. Lebedev Physical Institute, Russian Academy of Science (LPI RAS), Moscow, Russia

[b]Università di Bari, Bari, Italy
[c]Università di Bologna, Bologna, Italy
[d]Università di Cagliari, Cagliari, Italy
[e]Università di Ferrara, Ferrara, Italy
[f]Università di Firenze, Firenze, Italy
[g]Università di Urbino, Urbino, Italy
[h]Università di Modena e Reggio Emilia, Modena, Italy
[i]Università di Genova, Genova, Italy
[j]Università di Milano Bicocca, Milano, Italy
[k]Università di Roma Tor Vergata, Roma, Italy
[l]Università di Roma La Sapienza, Roma, Italy
[m]Università della Basilicata, Potenza, Italy
[n]LIFAELS, La Salle, Universitat Ramon Llull, Barcelona, Spain
[o]Hanoi University of Science, Hanoi, Viet Nam
[p]Associated to Universidade Federal do Rio de Janeiro (UFRJ), Rio de Janeiro, Brazil
[q]Associated to Physikalisches Institut, Ruprecht-Karls-Universität Heidelberg, Heidelberg, Germany